

Applying Deep Learning Techniques in Automated Analysis of Echocardiograms, CMRs and Phonocardiograms for the Detection and Localization of Cardiac Diseases

Arvind K. Bansal and Racheal Mukisa

Department of Computer Science
Kent State University
Kent, OH 44242, USA

email: akbansal@kent.edu and rmukisa1@kent.edu

Abstract— Echocardiography (echoCG), Cardiac Magnetic Resonance (CMR) and phonocardiograms (PCG) are becoming indispensable tools in the diagnostics and management of cardiac diseases due to advancements in imaging techniques, improvement in processing power, availability of large multimedia databases in Electronic Medical Records (EMR) and rapid lowering of cost. Image-based and video-based data in echoCG and CMR are multi-dimensional and exceed the capabilities of traditional statistical learning. Deep learning technologies provide new possibilities for accurate, consistent, and automated interpretation of echoCG, CMR, and PCG, reducing the risk of human error. Deep learning and signal analysis techniques are being applied to analyze these complex data for improved diagnosis of cardiac diseases involving heart muscles, valvular defects, cardiac chamber deformities negatively affecting blood-oxygenation and blood-flow. This review describes applications of deep learning techniques, such as Convolutional Neural Network (CNN), Recurrent Neural Network (RNN), Long Short-term Memory Neural Network (LSTM), transfer learning, and their variations in enhancing the classification of heart diseases from echoCG, CMR and PCG.

Keywords—Artificial Intelligence; CMR; deep learning; echocardiogram; heart diseases; machine learning; Phonocardiogram.

I. INTRODUCTION

The importance of Cardiovascular Diseases (CVD), Congenital Heart Diseases (CHD) and other heart-related diseases is significant. According to World Health Organization (WHO), 17.9 million persons died annually of CVD worldwide [1]. Total prevalence of cardiac diseases in 2018 was around 126.9 million USA alone [2]. Infants are born with CHD with a mean rate of 8.2 per thousand births per year worldwide [3]. Their long-term prognosis for survival is low. Invasive surgery is expensive, risky and not advisable for diagnostics and maintenance of heart-conditions post-surgery.

Electrocardiogram (ECG), echocardiogram (echoCG), Cardiac Magnetic Resonance (CMR) and digital phonocardiograms (PCG) are minimally invasive techniques that have been used to assess heart abnormalities [4]-[11]. Computer Tomography (CT) is also used to study heart

defects [8]. However, CT scans are associated with radiation and have lesser resolution than CMR [8].

ECG is the least invasive technique and suitable for indicating CVD affecting change in emitted waveforms. However, it is not well suited to assess localization of structural defects and motion-related deformities in heart-muscles (such as hypertrophic cardiomyopathy) and heart-valves (such as mitral valve regurgitation or aortal stenosis) and cannot assess blood-volume flow – an important feature to assess the heart diseases due to smaller volume of blood-flow, turbulent blood-flow, stenosis, mixing of oxygenated and deoxygenated blood due to holes in the septum, and ischemia caused by plaque formation and arteriosclerosis.

Due to improved resolution in inexpensive echoCGs, CT scans are less preferred and have been left out in this review. ECG analysis has been left out due to its limitations in localization of cardiac defects. In this paper, we review the applications of deep learning methods to analyze echoCG, CMR and PCG.

Recent progress in echoCG has made it quite accurate, inexpensive, and a preferred alternative for assessing structural and blood-flow-related diseases. CMR has the highest resolution. However, it is expensive. EchoCG is preferred to measure the speed of blood-flow and blood-turbulence present in many valvular diseases [4]. PCG is analyzed to diagnose limited cardiac diseases based upon emitted sound, while echoCG and CMR use images, image-sequences and video-clips of heart-muscles and valves [7][9]-[13].

Guidelines have been developed to ensure accurate interpretation of echoCG, CMR and PCG outputs [12]. However, the final analysis heavily relies on the operators' experience and knowledge. This causes subjectivity and variability in interpreting image and sound patterns [12].

In the last decade, image analysis and speech-recognition has improved significantly due to rapid advances in deep learning techniques, such as Convolutional Neural Network (CNN), Recurrent Neural Network (RNN), Long Short-term Neural Network (LSTM), transfer learning, and their variations and combinations. Deep Neural Networks (DNN) exploit convolution-filter-based feature-maps, temporal context, memory, and selective forgetfulness in the artificial neurons to improve object-classification [14]-[17].

AI and deep learning techniques are being exploited to generate accurate, consistent and automated interpretation of echoCGs, CMR and PCG to diagnose cardiac diseases related to structural and heart muscles related defects, valvular defects, and blood-flow-related diseases [4]–[6]. For example, machine learning models have been shown to provide an instantaneous assessment of the left ventricular ejection fraction and longitudinal strain [13].

Large volumes of multidimensional imaging data generated in 2D, 3D and 4D (includes 3D images and temporality present in video clips) formats are available (see Section VII). EchoCG requires image-classification and video-analysis; CMR requires analysis of 2D and 3D cardiac images and 4D videos. PCG requires waveform segmentation and analysis to classify the wave-patterns.

Many factors have contributed to the recent interest and the advancement of cardiac image and motion analysis: 1) multifold improvement in deep learning techniques in the last decade; 2) availability of large scale of high-resolution CMR and echoCG datasets; 3) lowering of the cost of CMR and echoCG; 4) recent acceptance of automated intelligent image analysis techniques by the clinicians in other disease domains such as mammograms; and 5) cost and side-effects of invasive exploration for cardiac diseases.

The rest of this paper is organized as follows. Section II describes the background concepts: heart anatomy, echoCG, CMR, and deep learning techniques. Section III describes diseases associated with defects and deformities in heart muscles, valvular (heart-valves related) and blood-flow-related diseases. Section IV describes echoCG analysis. Section V describes CMR analysis. Section VI describes PCG analysis. Section VII describes major data repositories. The last section concludes the discussion.

II. BACKGROUND

A. Heart Anatomy

A heart (see Figure 1) comprises four chambers: Left Atrium (LA); Right Atrium (RA); Left Ventricle (LV); Right Ventricle (RV). LA gets oxygenated blood from the lungs; LV pumps oxygenated blood to the body; RA collects deoxygenated blood from the body; RV sends deoxygenated blood to the lungs. The left and right sides are separated by a muscle called ‘septum’ [5]. A hole in the septum contaminates oxygenated blood in the LV (or LA) with deoxygenated blood in the RV (or RA).

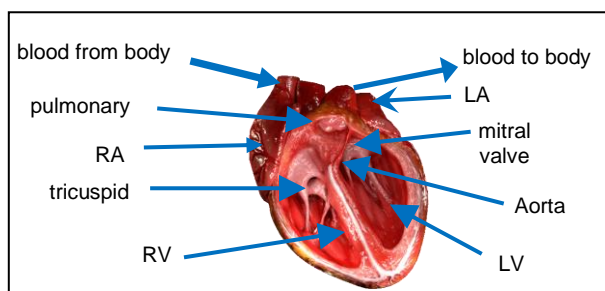


Figure 1. An illustration of heart anatomy [18].

A heart has four valves: 1) *aortic valve* regulating blood-flow from LV to the body; 2) *mitral valve* regulating blood-flow from LA to LV; 3) *pulmonary valve* regulating blood-flow from RV to lungs; 4) *tricuspid valve* regulating blood-flow from RA to RV. Valves comprise two or three leaflets that open and close synchronously. Periodic relaxation and compression of cardiac chambers cause blood flow. Two valves, *aorta* and *mitral*, play key roles in the oxygenated blood-flow from the heart to the body.

B. Echocardiogram

EchoCG (see Figure 2 [18]) is an ultrasound-based technique that assesses the reflectivity and refraction of emitted microwaves altered by tissue type and density [5]. There are two types of echograms: *transthoracic echoCG* (TTE) and *transesophageal echoCG* (TEE). TTE is a noninvasive and preferred technique [19].

By comparing the differences between signal reflected between the healthy tissue and the query tissue, the technique assesses the presence and the extent of unhealthy tissue layers and their thickness [8]. By combining echoCG with Doppler effect, blood-flow speed and direction are also estimated [16].

C. Cardiac Magnetic Resonance (CMR)

Cardiac Magnetic Resonance (CMR) is a high-resolution imaging technique using a strong magnetic field that excites hydrogen ions in water molecules inside tissues in a Region of Interest (ROI). CMR measures the emitted energy when hydrogen ions return to the normal state [8]. The relaxation time differs between healthy tissues and diseased tissues. By knowing the relaxation patterns of tissues, CMR images are formed. Pixels/voxels can be imaged [8] in an ROI by superimposing non-uniform magnetic-field with a static strong magnetic field,

Computational combinations of multiple slices of CMR in images give a 3D CMR image that is visualized using computer graphics. As shown in Figure 3 [21], CMR is used to analyze the deformities in different cardiac chambers, and changes in their motions and blood-flow patterns [8]-[11].

D. Phonocardiogram (PCG)

Phonocardiograms are high-fidelity sound recordings (see Figure 4 [22]) generated by continuous opening and closing of cardiac valves, and blood-flow through arteries in heart-chambers [7][23][24]. Different valvular diseases create different sound-patterns (see Figure 4) helping in the classification and identification of valvular diseases.

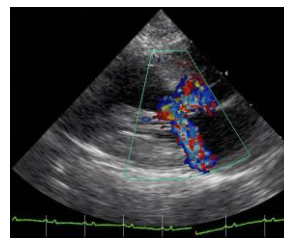


Figure 2. An illustration of echocardiogram [20].

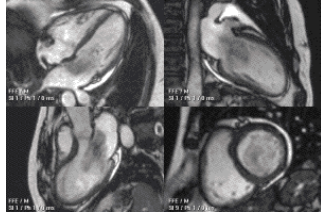


Figure 3. An illustration of CMR image [21].

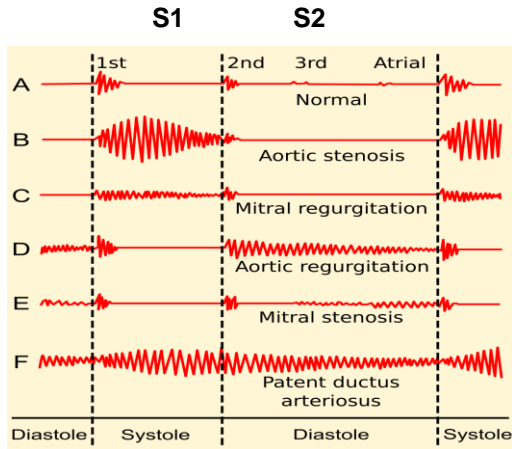


Figure 4. Phonocardiogram of different heart defects [22].

PCG comprises two major sound patterns S1 and S2, for each cardiac cycle, as shown in Figure 4. The sound S1 occurs at the beginning of the ventricular systole due to the closure of atrioventricular valves: *mitral* and *tricuspid*. The sound S2 marks the beginning of ventricular diastole and comprises two components due to the closure of *aortic* and *pulmonary* valves [7][23].

III. VALVULAR AND HEART MUSCLE DISEASES

Classes of cardiac disease derived using deep learning techniques are: 1) deformity in the heart-structure or the presence of a tumor; 2) calcification causing a lack of synchronization in heart-valves resulting in blood-leak (stenosis), or regurgitation in the corresponding blood channels; 3) thickening of cardiac walls in one or more chambers reducing the blood-flow volume and negatively affecting the heart-motion; 4) plaque formation in an artery or vein restricting blood-flow [4][9][13][19].

Deformities in the valves cause *stenosis* - restricting the blood-flow, or *regurgitation* - turbulent blood-flow and/or blood-flow in reverse direction around a valve. Four classes of valvular diseases have been computationally analyzed using DNN in recent years [4][19]. The diseases are *aortic stenosis*, *mitral stenosis*, *aortic regurgitation*, and *mitral regurgitation*. Uneven calcifications on valve-leaflets cause a lack of synchronization in the opening and closing of valves resulting in regurgitation and stenosis [4].

Another valvular disease is *Rheumatic Heart Disease* (RHD) that occurs as an after-effect of rheumatic fever, resulting in valvular lesions in aorta valve, mitral valve or tricuspid valve, weakening the valve-function. Affected

valves develop regurgitation and stenosis, with the most common being *mitral regurgitation* [4][19].

Another class of disease is *Congenital Heart Diseases* (CHD) where the cardiac structure has defect(s) since birth [18][19]. Common CHDs are: 1) *Congenital Valve Disease* (CVD), including *Bicuspid Aortic Valve Disease* (BAVD), *Pulmonary Valve Stenosis* (PVS), *Aortic Valve Stenosis* (AVS), and *Ebstein’s anomaly*; 2) *Atrial Septal Defect* (ASD) – a hole in the septum between upper chambers connecting LA and RA; 3) *Ventricular Septal Defect* (VSD) – a hole in the septum in lower chambers connecting LV and RV; 4) *Coarctation of the aorta* (CA) – narrowing of the aorta after it leaves the heart causing blood-turbulence; 5) *Patent Ductus Arteriosus* (PDA) - connection between two blood channels because channels do not close after birth (see Figure 5 [26]).

Ebstein’s anomaly is a severe heart defect in leaflets of a *tricuspid valve* (between RA → RV) restricting blood-flow to lungs, resulting into the lack of oxygenation. *Tetralogy of Fallot* is a combination of four CHDs: *VSD*, *PVS*, a *misplaced aorta* and *right ventricular hypertrophy*. It causes the lack of blood-flow and deoxygenation of blood, resulting in ischemia and vascular degeneration.

Other muscle-related conditions are *cardiac myopathy* (thickening of heart muscles) and *cardiac hypertrophy* (smaller volume in heart chambers due to the thickening of cardiac walls) [8]. *Myopathy* causes heart chambers to contract slowly, reducing the blood-flow [13][19]. *Cardiac hypertrophy* is accompanied by *myopathy* [8]. *Cardiac hypertrophy* is identified by analyzing the wall-thickness combined with the ejection-volume estimation from the LV.

Applications of deep learning techniques for diagnosing cardiac muscles-related and valvular diseases are summarized in Table I.

IV. ECHOCARDIOGRAM ANALYSIS

EchoCG analysis can diagnose valvular diseases, such as *stenosis* and *regurgitation*, *atrial blockages*, *atrial fibrillation*, *congenital heart disease*, *coronary arterial disease*, *cardiomyopathy*, *cardiac hypertrophy*, and *murmur* [19][25][28]-[32].

TABLE I. DNN LEARNING BASED ANALYSIS FOR CARDIAC DISEASES

Disease Class	Input Mode	DNN Technique
Valvular stenosis + regurgitation	echoCG and PCG	CNN-based segmentation and TGNN + CNN + LSTM
Fetal heart defects	echoCG + CMR	CNN-based segmentation for wall boundaries
Myocardium hypertrophy and myopathy	Doppler echoCG + CMR	Hybrid CNN + LSTM + encoders and decoders for wall thickness, chamber boundaries and blood flow volume
Ischemia and myocardial infarction	CMR	CNN based tissue classification

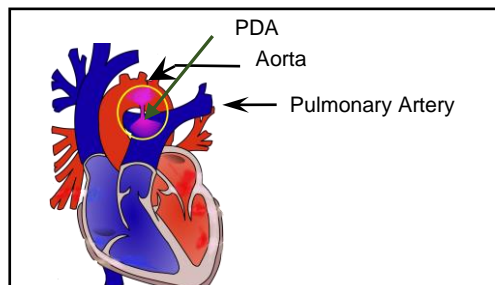


Figure 5. An illustration of PDA [26].

Aortal and mitral valve regurgitations have been identified using R-CNN (region-based CNN) on color Doppler echoCG [19]. R-CNN uses a bounding rectangular box around the objects and uses a combination of CNN and Support Vector Machine (SVM) for classification and object-detection [17]. Regurgitation is estimated semi-quantitatively using jet-area ratios. The area of an orifice is measured using ‘proximal flow convergence’ of blood-flow measured using Doppler effect [32].

Segmentation for valvular regurgitation uses multiple techniques, such as non-linear anisotropic diffusion [8][32]. *Regurgitation* is estimated using *Proximal Isovelocity Surface Area (PISA)*, which occurs when fluid flows through a circular orifice [33]. As fluid passes through a narrow orifice, it speeds up that can be measured.

CHDs have been identified using multiview (five views) echoCG analysis using multichannel CNN [25]. The advantage of having multiple views is clarity and supporting evidence from other views [19][25]. To reduce overfitting due to the limited availability of data, *depth-wise separable convolution* has been used. A standard convolution filter combines inputs in the same step. *Depth wise convolution* filters and combines in two separate layers, reducing the computational complexity.

Video of each view is fed to an encoder for frame-independent feature representation. It uses RNN to assign different weights to frames with the highest weight to the most relevant frame and progressively reduces weights for its neighbors. It uses *temporal convolution* to identify the neighboring frames [34]. *Temporal convolutions* are used on time-series data to maintain temporality and causality.

Common fetal heart defects are: (1) *tetralogy of Fallot*; (2) *ventricular dysplasia*; (3) *Ebstein’s anomaly*. The major problem in a fetal heart defect is the malformation of a subset of cardiac chambers and the leakage between the chambers due to holes in the septum. Major problems in the identification of cardiac chambers from infants’ echoCGs are: 1) artifact; 2) discrimination between chambers; 3) missing boundaries. The physical boundaries between atrium and ventricles are missing when the corresponding valves are opening. This requires deep learning techniques for echoCG analysis to identify four chambers and their motions accurately using segmentation.

Researchers have developed a cascaded dual layered Deep Wide Neural Network (DW-net) for semantic

segmentation of echoCGs [35]. DW-net comprises two layers: (1) Dilated Convolutional Chain (DCC) and W-net. DCC collects local and global features for the localization of ROI. W-net derives precise boundaries in ROI by repeated applications of encoders and decoders.

EchoNet, a CNN based model, detects cardiac structure and anatomy, blood-flow volume, the presence of pacemakers, LV hypertrophy, enlargement of LA chamber along with the prediction of age, sex, and gender of a patient [33]. It is trained on a large feature-set comprising age, sex, weight, BMI, presence of a pacemaker, LA enlargement, LV hypertrophy, End Systolic Volume (ESV), End Diastolic Volume (EDV), and Ejection Fraction (EF) [33].

V. CMR ANALYSIS

CMR imaging is a reference for imaging due to higher resolution. The cardiac region is identified knowing that heart movements change voxel-intensities in the dynamic part of a heart. LV, being the largest moving chamber, has been targeted for segmentation. LV also circulates maximum blood volume. After a ROI is identified, segmentation techniques are applied to derive the LV. After identifying the LV region, model-based techniques, augmented with deep learning techniques, derive other chambers and boundaries.

CMR analysis is also applied to estimate EDV, ESV, EF, and Myocardial Mass (MM) [36][37]. This quantification has been used to study blood ejection from each chamber, especially LV, and has been used to estimate the extent of cardiac myopathy and cardiac hypertrophy [37][38].

A major problem in CMR analysis is the segmentation of various boundaries in the heart to detect chambers, valves, artery, septum, muscles and valvular defects, especially in the presence of variations of pathologies in different patients. Segmentation approaches are image-driven or model-driven [37]. The image-driven approach uses intensity-based histogram analysis and thresholding, clustering, region growing, pixel/voxel level classification and active contours to identify blood-pool, myocardium or appendages. The model-based approach uses statistical analysis to derive atlas or shape contours.

The segmentation methods are classified as pixel-level classification, graph-based methods, probabilistic models, such as Markov Random Fields, deformity-based models, atlas-based methods, CNN and LSTM based deep learning models, and hybrid techniques that integrate deep learning techniques and deformity-based models [39][40]. Deformity-based models are based upon shape estimation. However, pixel-level classification, shape-based models, including deformity-based models (shape contours), and probabilistic models suffer from inaccuracies [40]. Random forest models are based on intensity classification that causes inaccuracy. Combined with deep learning models, deformity-based models accurately estimate the dynamic shape of various chambers [40].

LV segmentation has been used to derive motion estimation, wall thickness on different sides, local deformation and myocardial strain during systole and diastole phases [37]. Wall thickness changes for an ischemic heart [38]. Wall thickness in the LV during the systole phase

is used to estimate malfunction in myocardial ischemia or myocardial infarction. Most of the clinical assessment is done qualitatively by visual assessment [38]. Quantitatively, a LV strain indicates deformation of the ventricles, which is used as a parameter in Doppler echoCG analysis to estimate the extent of ischemia, myocardial infarction, and ventricular dyssynchrony.

The LV End-diastole Volume (LVEDV) and the LV End-systole Volume (LVESV) are used to estimate the LV Stroke Volume (LVSV) - the total ejection rate from the LV in each cycle. The Left Ventricle Ejection Fraction (LVEF) is derived by dividing LVESV by LVEDV. LVEF quantifies the fraction of blood pumped out by the LV in each cycle [37].

One technique to derive the LV region is the application of the Hough transform at the end of diastole and model the region using concentric circles. The region showing the maximum projected intensity near the center of concentric circles is a viable candidate for the LV seed [37]. Other properties of the LV region are homogeneity and high grey level. The segmentation, identification techniques, and quantification techniques for other chambers are similar.

CMR images are acquired using fixed periodic time after the occurrence of R-waveforms – the most prominent waveform in ECG associated with the compression of the LV. Patients with arrhythmia have varying heart-cycle which degrades the image quality. There are challenges because different chambers and walls have similar intensity profile, making contrast-based segmentation difficult [39]. Artifacts, noise, lighting conditions and heterogeneity due to blood-flow also affect the intensities [39][40].

VI. PCG ANALYSIS

PCG analysis is based upon signals derived from systolic and diastolic phases of blood-flow turbulence to estimate the occurrence of valvular diseases like stenosis, regurgitation, atherosclerotic disease, and murmur (see Figure 4) [23][41]. However, unlike image-based techniques, PCG cannot accurately localize valvular and muscle-deformity-related diseases, such as myopathy or hypertrophy, and diseases related to blood-leakage.

PCG analysis requires signal analysis in the time-domain using discrete wavelet or packet wavelet transforms [23] or in frequency domain using FFT [27].

Intelligent PCG uses *Time Growing Neural Network* (TGNN) based analysis to segment the time-series of diastolic and systolic sound patterns of stenosis of aortic, pulmonary and tricuspid valves [42]. TGNN combines windowing to extract signal frames with neural network for the classification. Windowing uses a fixed starting point but growing endpoints to identify varying size time-framed windows containing the signal.

A hybrid model combining CNN and LSTM has been used for the classification of PCG [43]. CNN is used to analyze the frequency-related features derived using *Mel Frequency Cepstral Coefficient* (MFCC), and LSTM is used to derive temporal dependencies. Another research combined CNN and bidirectional LSTM to detect aortic

stenosis, mitral stenosis, mitral regurgitation, and mitral valve pro-lapse [44].

VII. MAJOR DATASETS

EchoNet-Dynamic database contains 10,030 labeled apical-4-chamber echocardiography videos and human expert annotations in the form of measurements, tracings, and calculations to study cardiac motion and chamber sizes [45][46]. Data is accompanied by EF values of LV and frame numbers of end-systole and end-diastole frames determined by medical practitioners.

CREATIS repository provides multimodal 2D and 3D cardiac imaging data, application-software, and diagnostics to evaluate computational methods and enhance collaboration around heart imaging and analysis [47]. The repository is a collection of multiple databases: 1) *CAMUS synthetic database* contains 2D apical myocardial motion in four chambers; 2) *Duplex database* contains twenty simulated sequences; 3) *Cetus database* contains 3D echoCG sequences of 45 clinical patients; 4) *Multimodal Straus database* contains 3D echoCG data, cine-MRI and tagged-MRI data of eighteen virtual patients; 5) *Revolus database* contains 2D echoCG of both simulated and actual sequences; 6) *ACDC database* contains 3D CMR data along with manual contouring to mark LV endocardium and RV endocardium for both diastolic and systolic phases; 7) *Minimalist Immediate Mechanical Intervention (MIMI) dataset* comprises a multicentric randomized trial comparing immediate and delayed stenting in 140 patients treated with *Percutaneous Coronary Intervention* (PCI).

The *Harvard dataverse* comprises cardiac imaging datasets, such as CMR images of 35 patients with mitral regurgitation, 4D-flow echoCG image-sequence, and CMR data from 108 subjects (patients and healthy subjects) [48].

The *Heart database* comprises 3D CMR images of LV with automated segmentations validated by clinicians, tools to compute quantitative measures, and software packages for automated image segmentation [49].

The *EMIDEC database* comprises datasets for classifying normal and pathological cases of 150 MRI exams from different patients for studying LV in the cases of myocardial infarction symptoms [50].

The *Physionet database* contains nine PCG databases and applied deep neural networks to classify heart murmurs [51].

The *Cardiac Atlas Project (CAP) database* contains data of asymptomatic and pathological hearts to facilitate collaborative statistical analysis of regional heart shapes and characterize cardiac function for multiple population groups [52].

VIII. DISCUSSION AND CONCLUSION

This review has described the trend of applying deep learning techniques for cardiac image segmentation needed for detecting cardiac chambers, blood-channels, blood-flow and its quantification, and its various defects, such as heart muscle deformation, plaque formation, calcification and valvular defects. It also describes the combination of frame

segmentation and deep learning networks to classify sounds collected in PCG.

The advantage of deep learning is in identifying feature-maps due to intensity and texture variations using convolution layers, and repeated patterns of encoders and decoders, providing temporality as required in analyzing various phases of blood-flow, sound generation and heart-muscle movements in heart cycles. CMR and echoCG images contribute to the better quantification-based image analysis. Traditional quantification techniques such as blood-flow estimates, augmented with deep learning-based boundary detection and strain detection have significantly improved the diagnosis and the classification of heart-defects.

The drawbacks in image analysis are the presence of noise such as speckles due to blood-flow that hinder segmentation, inability to separate similar defects such as ischemic and infarcted regions, inaccurate detection of boundaries of wall chambers, especially when the valves are open. Another drawback is the absence of a large dataset required to improve the accuracy in deep learning techniques. This problem is being resolved progressively, as described in Section VII. Despite clinical validation of results, a major criticism of a deep learning model is the black box approach with no causality-based explanation.

In the next decade, deep learning techniques, combined with continuously reducing cost of use, will be established as a valuable tool for automated diagnostics and fast and accurate decision support system to identify noninvasively the extent and localization of the muscle, motion and valves related cardiac diseases.

REFERENCES

- [1] World Health Organization Facts Sheet, available at [https://www.who.int/news-room/fact-sheets/detail/cardiovascular-diseases-\(cvds\)](https://www.who.int/news-room/fact-sheets/detail/cardiovascular-diseases-(cvds)), last accessed April 30, 2022.
- [2] S. S. Virani, A. Alonso, H. J. Aparicio, E. J. Benjamin, M. S. Bittencourt, C. W. Callaway et al., "Heart Disease and Stroke Statistics – 2021 Updates," *Circulation*, vol. 143, No. 8, pp. e254-e742, Feb. 2021, doi: 10.1161/CIR.0000000000000950.
- [3] D. V. D. Linde, E. E. M. Konings, M. A. Slager, M. Witsenburg, W. A. Helbing et al., "Birth Prevalence of Congenital Heart Disease Worldwide: A Systematics Review and Meta-analysis," *Journal of American College of Cardiology*, vol. 58, issue 21, pp. 2241-2247, Nov. 2011, doi: 10.1016/j.jacc.2011.08.025.
- [4] K. Maganti, V. H. Rigolin, M. E. Sarano, and R. O. Bonow, "Valvular Heart Disease: Diagnosis and Management," *Symposium on Cardiovascular Diseases, Mayo Clinic Proceedings*, vol. 85, issue 5, pp. 483-500, May 2010, doi: 10.4065/mcp.2009.0706.
- [5] S. J. Al'Aref, K. Anchouche, G. Singh, P. J. Slomka, K. K. Kollu, A. Kumar et al., "Clinical Applications of Machine Learning in Cardiovascular Disease and its Relevance to Cardiac Imaging," *European Heart Journal*, vol. 40, pp. 1975-1986, 2019, doi: 10.1093/eurheartj/ehy404.
- [6] B. Xu, D. Kocyigit, R. Grimm, B. P. Griffin, and F. Cheng, "Applications of Artificial Intelligence in Multimodal Cardiovascular Imaging: A State of Art Review," *Progress in Cardiovascular Diseases*, vol. 63, pp. 367-376, 2020, doi: 10.1016/j.pcad.2020.03.003.
- [7] A. G. Tilkian and M.B. Conover, *Understanding Heart Sounds and Murmurs: With an Introduction To Lung Sounds*, fourth ed., Saunders: Philadelphia, PA, 2001.
- [8] A. K. Bansal, J. I. Khan, and S. K. Alam, "Introduction to computational health informatics," CRC Press: Newyork, NY, 2020, doi: 10.1201/9781003003564.
- [9] S. G. Myerson, J. Francis, and S. Neubauer, *Cardiovascular magnetic resonance*, Oxford University Press: Oxford, UK:, 2013.
- [10] T. Rogers and R. Waksman, "Role of CMR in TAVR," *JACC: Cardiovascular Imaging*, vol. 9, No. 5, pp. 593-602, May 2016, doi: 10.1016/j.jcmg.2016.01.011.
- [11] A. S. Fahmy et al. "Automated cardiac MR scar quantification in hypertrophic cardiomyopathy using deep convolutional neural networks," *JACC Cardiovasc Imaging*, 2018, vol. 11, pp. 1917–18, doi: 10.1016/j.jcmg.2018.04.030.
- [12] F. C. Cobey, V. Patel, and A. Gosling, "The Emperor has no Clothes: Recognizing the Limits of Current Echocardiographic Technology in Perioperative Quantification of Mitral Regurgitation," *Journal of Cardiothoracic and Vascular Anesthesia*, vol. 31, issue 5, pp. 1692-1694, Oct. 2017, doi: 10.1053/j.jvca.2017.03.012.
- [13] C. Knackstedt, S. C. A. M. Bekkers, G. Schummers, M. Schreckenberg, D. Muraru, I. P. Badano et al., "Fully Automated versus Standard Tracking of Left Ventricular Ejection Fraction and Longitudinal Strain: the FAST-EFs Multicenter Study," *Journal of the American College of Cardiology*, vol. 66, no. 13, pp. 1456-1466, Sept. 2015, doi: 10.1016/j.jacc.2015.07.052.
- [14] S. Russel and P. Norvig, "Artificial Intelligence – A Modern Approach," 4th Edition, Pearson Education: Hoboken, NJ, 2020.
- [15] Y. LeCun Y. Bengio, and G. Hinton, "Deep learning," vol. 521, issue 7553, pp. 436-444, May 2015, doi: 10.1038/nature14539.
- [16] L. Deng and D. Yu, "Deep learning methods and applications," *Foundations and Trends in Signal Processing*, vol. 7, issue 3-4, pp. 197-387, June 2014, doi: 10.1561/20000000039.
- [17] Z.-Q. Zhao, P. Zheng, S.-T. Xu, and X. Wu, "Object Detection with Deep Learning – A Review," *IEEE Transactions of Neural Networks and Learning Systems*, vol. 30, no. 11, pp. 3212-3232, Nov. 2019, doi: 10.1109/TNNLS.2018.2876865.
- [18] Computer generated cross-section 3D model of heart, Wikimedia Commons, Creative License 4.0, available at https://commons.wikimedia.org/wiki/User:DrJanaOfficial#/media/File:CG_Heart.gif, last accessed May 16, 2022.
- [19] Q. Jhang, Y. Liu, J. Mi, X. Wang, X. Liu, F. Zhao et al., "Automatic Assessment of Mitral Regurgitation Severity Using the Mask R-CNN Algorithm with Color Doppler Echocardiography Images," *Computational and Mathematical Methods in Medicine*, vol. 2021, Article Id: 2602688, pp. 1-10, Sept. 2021, doi: 10.1155/2021/2602688.
- [20] Ekko, Ventricular septal defect, Wikimedia Commons, Public domain, available at https://commons.wikimedia.org/wiki/File:Ventricular_Septal_Defect.jpg, last accessed May 16, 2022.
- [21] J. C. C. Moon and M. danne, A CMR image of a benign tumor in a heart, Wikimedia Commons, available at https://commons.wikimedia.org/wiki/File:Myxoma_CMV.gif, last accessed May 16, 2022.
- [22] Phonogram from normal and abnormal heart, Wikimedia Commons, GNU free documentation, License 1.2, https://commons.wikimedia.org/wiki/File:Phonocardiograms_from_normal_and_abnormal_heart_sounds.png#/media/File:P

- honocardiograms_from_normal_and_abnormal_heart_sounds.svg, last accessed May 16, 2022.
- [23] L. H. Cherif, S.M. Debbal, and F. Bereksi-Reguig, "Choice of the Wavelet Analyzing in the Phonocardiogram Signal Analysis using the Discrete and Packet Wavelet Transforms," *Expert Systems with Applications*, vol. 37, issue 2, pp. 913-918, March 2010, doi: 10.1016/j.eswa.2009.09.036.
- [24] F. Kovács, C. Horváth, A. T. Balogh, and G. Hosszú, "Fetal Phonocardiography – Past and Future Possibilities," *Computer Methods and Programs in Biomedicine*, vol. 104, issue 1, pp. 19-25, Oct. 2011, doi: 10.1016/j.cmpb.2010.10.006.
- [25] J. Wang et al., "Automated Interpretation of Congenital Heart Disease from Multi-view Echocardiograms," *Medical Image Analysis*, vol. 69, Article 101942, pp. 1-12, 2021, doi: 10.1016/j.media.2020.101942.
- [26] An illustration of PDA, Wikimedia Commons, Public domain, Available at https://en.wikipedia.org/wiki/Patent_ductus_arteriosus#/media/File:Patent_ductus_arteriosus.svg, last accessed May 16, 2022.
- [27] Z. Abduh, E. A. Neharyb, M. A. Waheda, and Y. M. Kadaha, "Classification of Heart Sounds using Fractional Fourier Transform based Mel-Frequency Spectral Coefficients and Traditional Qualifiers," *Biomedical Signal Processing and Control*, vol. 57, Article Id 101788, pp. 1-11, 2020, doi: 10.1016/j.bspc.2019.101788.
- [28] Z. Akkus et al., "Artificial Intelligence (AI) Empowered Echocardiography Interpretation – A State of Art Review," *Journal of Clinical Medicine*, vol. 10, issue 7, Article Id 1391, pp. 1-16, doi: 10.3390/jcm1007139.
- [29] L. Xu, M. Liu, Z. Shen, H. Wang, X. Liu, and X. Wang, "DW-net a Cascaded Convolution Network for Apical Four-chamber View Segmentation in Fetal Echocardiography," *Computerized Medical Imaging and Graphics*, vol. 80, Article 101690, pp. 1-11, March 2020, doi: 10.1016/j.compmedimag.2019.101690.
- [30] R. Nedadur, B. Wang, and W. Tsang, "Artificial Intelligence for the Echocardiographic Assessment of Valvular Heart Disease," *Heart*, Article Id 319725, pp. 1-8, Feb. 2022, doi: 10.1136/heartjnl-2021-319725.
- [31] I. Wahlang et al., "Deep Learning Methods for Classification of Certain Abnormalities in Echocardiography," *Electronics*, vol. 10, Article 495, pp. 1-20, Feb. 2021, doi: 10.3390/electronics10040495.
- [32] A. K. Pinjari, P. V. Sridevi, and M. N. GiriPrasad, "Segmentation Methods for Severity Regurgitation: A Comparative Analysis," *Research Journal of Recent Sciences*, vol. 3, no. 6, pp. 83-89, June 2014, available at www.isca.in/rjrs/archive/v3/i6/13.ISCA-RJRS-2014-833.pdf.
- [33] A. Ghorbani et al., "Deep Learning Interpretations of Echocardiograms," *NPJ Digital Medicine*, vol. 3, Article 10, pp. 1-10, Jan. 2020, doi: 10.1038/s41746-019-0216-8.
- [34] S. Bai, J. Z. Kolter, and V. Koltun, "An empirical evaluation of generic convolutional and recurrent networks for sequence modeling," *arXiv preprint, arXiv:1803.01271*, pp. 1-14, April 2018, doi: 10.48550/arXiv.1803.01271.
- [35] L. Xu et al. "DW-Net: A Cascaded Convolutional Neural Network for Apical Four-chamber View Segmentation in Fetal Echocardiography," *Computerized Medical Imaging and Graphics*, vol. 80, Article Id. 101690, pp. 1-11, March 2020, doi: 10.1016/j.compmedimag.2019.101690.
- [36] C. Constantinides, E. Roullot, M. Lefort, and F. Frouin, "Fully Automated Segmentation of the Left Ventricle Applied to Cine MR Images: Description and Results on a Database of 45 Subjects," 34th Annual International Conference of the IEEE EMBS, San Diego, CA, USA, Aug.-Sept. 2012, pp. 3207-3210.
- [37] P. Peng, K. Lekadir, A. Gooya, L. Shao, S. E. Petersen, and A. F. Frangi, "A Review of Heart Chamber Segmentation for Structural and Functional Analysis using Cardiac Magnetic Resonance Imaging," *Magn Reson Mater Physics*, vol. 29, issue 2, pp. 155-195, April 2016, doi: 10.1007/s10334-015-0521-4.
- [38] T. Emrich, M. Halfmann, U. J. Schoepf, and K.-F. Kreitner, "CMR for Myocardial Characterization in Ischemic Heart Disease: State of Art and Future Developments," *European Radiology Experimental*, vol. 5, issue 14, pp. 1-13, doi: 10.1186/s41747-021-00208-2.
- [39] L. V. Romaguera, F. P. Romero, C. F. C. Filho, and M. G. Fernandes, "Myocardial Segmentation in Cardiac Magnetic Resonance Images using Fully Convolved Neural Networks," *Biomedical Signal Processing and Control*, vol. 44, pp. 48-57, July 2018, doi: 10.1016/j.bspc.2018.04.008.
- [40] M.R. Avendi, A. Kheradvar, and H. Jafarkhani, "A Combined Deep-learning and Deformable-model Approach to Fully Automatic Segmentation of the Left Ventricle in Cardiac MRI," *Medical Image Analysis*, vol. 30, pp. 108-119, May 2016, doi: 10.1016/j.media.2016.01.005.
- [41] Z. Tariq, S. K. Shah, and Y. Lee, "Automatic Multimodal Heart Disease Classification using Phonocardiogram Signals," *IEEE International Conference on Big Data, Virtual*, Dec. 2020, pp. 3514-3521.
- [42] A. Gharehbaghi, M. Lindén, and A. Babic, "An Artificial Intelligent based Model for Detecting Systolic Pathological Patterns of Phonocardiogram based on Time-growing Neural Network," *Applied Soft Computing Journal*, vol. 83, Article Id 105615, pp. 1-12, Oct. 2019, doi: 10.1016/j.asoc.2019.105615.
- [43] A. N. Netto and L. Abraham, "Detection and Classification of Cardiovascular Disease from Phonocardiogram using Deep Learning Models," *Second International Conference on Electronics and Sustainable Communication Systems (ICESC)*, 2021, pp. 1646-1651, doi: 10.1109/ICESC51422.2021.9532766.
- [44] M. Alkhodari and L. Fraiwan, "Convolutional and recurrent neural networks for the detection of valvular heart diseases in phonocardiogram recordings," *Computer Methods and Programs in Biomedicine*, vol. 200, Article Id. 105940, pp. 1-25, March 2021, doi: 10.1016/j.cmpb.2021.105940.
- [45] Echonet Dynamic Database. [Online]. Available from: <https://echonet.github.io/dynamic/index.html>.
- [46] D. Ouyang et al., "Video-based AI for beat-to-beat assessment of cardiac function." *Nature*, vol. 580, no. 7802, pp. 252-256, March 2020, doi: 10.1038/s41586-020-2145-8.
- [47] CREATIS – Human Heart Project Databases. [Online]. Available from: <http://humanheart-project.creatis.insa-lyon.fr/databases.html>.
- [48] A. Fahmy et al. Harvard dataverse. [Online]. Available from: <https://dataverse.harvard.edu/dataverse/cardiaccmr>.
- [49] J. Cousty et al., The 4D Heart database, [Online]. Available from: <https://www.laurentnajman.org/heart/index.html>.
- [50] EMIDEC- Automated Evaluation of Myocardial Infarction from Delayed-Enhancement Cardiac MRI database. [Online]. Available from: <http://emidec.com/>.
- [51] Physionet database. [Online]. Available from: <http://www.physionet.org>.
- [52] C. G. Fonseca et al., "The Cardiac Atlas Project—an imaging database for computational modeling and statistical atlases of the heart," *Bioinformatics*, vol. 27, no. 16, pp. 2288-2295, Aug. 2011, doi: 10.1093/bioinformatics/btr360.